EUROPEAN JOURNAL OF PURE AND APPLIED MATHEMATICS
2026, Vol. 19, Issue 2, Article Number 7140
ISSN 1307-5543 – ejpam.com
Published by New York Business Global

Sensitivity Analysis and Chaos Control of Stochastic Time Delay Haemorrhagic Conjunctivitis Disease

Aqeel Ahmad[1], Muhammad Faheem[1], Hung Minh Nguyen[2], Dilber Uzun Ozsahin[3,4,5], Hijaz Ahmad[5,6,7,*], Waleed Mohammed Abdelfattah[8,9], Muhammad Saeed Akram[1]

[1] *Department of Mathematics, Ghazi University D. G. Khan 32200, Pakistan*
[2] *Center for Pharmaceutical Biotechnology, College of Medicine and Pharmacy, Duy Tan University, Da Nang 55000, Vietnam*
[3] *Department of Medical Diagnostic Imaging, College of Health Science, University of Sharjah, 27272 Sharjah, United Arab Emirates*
[4] *Research Institute for Medical and Health Sciences, University of Sharjah, 27272 Sharjah, United Arab Emirates*
[5] *Irfan Suat Gunsel Operational Research Institute, Near East University, Nicosia/TRNC, Mersin 10, 99138, Turkey*
[6] *VIZJA University, Okopowa 59, 01-043 Warsaw, Poland*
[7] *Department of Mathematics, College of Science, Korea University, 145 Anam-ro, Seongbuk-gu, Seoul 02841, South Korea*
[8] *College of Engineering, University of Business and Technology, Jeddah 23435, Saudi Arabia*
[9] *Department of Engineering Mathematics and Physics, Faculty of Engineering, Zagazig University, P.O. Box 44519, Egypt*

Abstract. This work presents a stochastic model for the dynamics of hemorrhagic conjunctivitis, incorporating vaccination and time delay. The model examines asymptomatic and symptomatic outcomes, the impact of vaccination on individuals with inadequate immunity, and the role of temporal delays in infection control. Equilibrium points of the $C_sC_eC_vC_iC_r$ system are analyzed using qualitative and quantitative methods, including reproductive analysis and sensitivity-based verge conditions. Existence, constructive existence, and uniqueness are established for non-local operators, ensuring reliable epidemic modeling. The Caputo fractional operator and its constrained approximate solutions are employed for continuous disease monitoring, with MATLAB simulations demonstrating the effects of viral control measures and time delays for specific conjunctivitis strains. A stochastic extension of the deterministic model is developed to explore differences in dynamics and better understand epidemic phenomena.

*Corresponding Author.
DOI: https://doi.org/10.29020/nybg.ejpam.v19i2.7140

Email addresses: aqeelahmad.740@gmail.com (A. Ahmad), faheemarain316@gmail.com (M. Faheem), hungmolbio@gmail.com (H. M. Nguyen), dozsahin@sharjah.ac.ae (D. U. Ozsahin), hijazahmad@korea.ac.kr (H. Ahmad), w.abdelfattah@ubt.edu.sa (W. M. Abdelfattah), mrsaeedakram@gmail.com (M. S. Akram)

1. Introduction

Conjunctivitis, an inflammation of the conjunctiva, is another term for pink eye. The thin, translucent tissue covering the white portion of the eye and the inside of the eyelid is called the conjunctiva. It is a very contagious disease that causes a lot of tears, pain, redness, and yellow discharge. As said, allergies and irritants can also cause pink eye, but bacterial and viral infections are the most common causes. Microorganisms that can cause bacterial conjunctivitis include Streptococcus pneumonia, Hemophilus influenza, and Staphylococcus aurous. But this type of conjunctivitis usually does not have an infectious latent period and usually appears shortly after contact with those bacteria, exhibiting symptoms including crusty eyelids, pain, and the seeping of yellow or green substance [1, 2].

The use of mathematics in biological studies dates back to the early 13th century, when Fibonacci introduced his famous sequence to describe population growth. The term biomathematics was later introduced by Johannes Reinke in 1901. Building on this foundation, Daniel Bernoulli utilized mathematical principles to explain how various factors influence the structure of microscopic organisms. In essence, biomathematics involves the theoretical study of mathematical models to explore the fundamental principles governing the behavior and structure of biological systems [3]. Over the past several decades, the biological sciences have expanded dramatically, and it is realistic to assume that this trend will continue in light of considerable technological advancements. Society has consistently profited from mathematics and been able to make important contributions thanks to it. The natural sciences have greatly benefited from mathematics, and biological research may be altered by it as well [4]. We may be able to comprehend the astounding complexity of life better by using mathematical models. Specifically, these mathematical models are evaluated in turn by biology. Advances in computer algebra systems are making it easier to solve complex mathematical problems. Consequently, researchers may now focus on comprehending mathematical biology rather than trying to solve problems [5, 6].

Many biological, physical, and exobiological processes can now be mathematically simulated, which is becoming more and more common. The growing interest in this field is largely driven by the ability of mathematical models to account for complex and interacting factors that influence biological systems. Mathematical biology, a specialized branch of mathematics, has gained significant attention from researchers particularly in areas such as infectious disease modeling and conjunctivitis virus [7, 8]. The widespread application of mathematical models to build fundamental frameworks has greatly enhanced our understanding of the intricate nature of biological processes. In the study of infectious diseases, mathematical modeling plays a vital role in determining critical threshold levels, clarifying transmission mechanisms, and formulating effective control measures of conjunctivitis virus [9, 10]. Its use has proven highly valuable, offering practical insights for both the prevention and treatment of viral infections. Thus, mathematical modeling serves as a powerful and complementary tool in combating viral outbreaks [11].

Effective measures to limit the transmission of conjunctivitis include the use of antibiotic eye drops, maintaining strict hygiene practices, isolating infected individuals, and allowing

the infection to resolve naturally typically within two to three weeks. The disease is more prevalent in tropical regions [12, 13], and outbreaks often occur during the rainy season when the humid environment fosters viral growth utilization of reproductive number [14]. This trend is particularly evident in tropical countries such as Thailand, where isolation of affected individuals is essential to prevent further spread [15]. Granting sick leave for home isolation not only accelerates recovery but also minimizes the frequency and duration of potential infectious contacts under compain model [16]. The American Academy of Pediatrics likewise advises that adolescents remain home from school to avoid close contact with others and slow the rapid transmission of the virus. Furthermore, the development and application of mathematical models have significantly enhanced our understanding of conjunctivitis dynamics. Several notable studies [17–20] have contributed valuable insights into the mathematical modeling and understanding of different infections and viruses.
When studying infectious disease models, time delays are essential for evaluating sickness residence durations, treatment delays, and detection intervals. According to Pathak and Kota, time-delayed epidemic models offer a more realistic simulation of disease propagation because they take into consideration the intrinsic delays that occur during transmission and disease management operations including fuzzy logic [21]. Determining the true pace of sickness progression and the effects of medication response from these stages, however, can occasionally be difficult. These interpolations and missing data points could miss immune response time delays because of the potential for an exponential rate of disease transmission. time delays in the immune response to viral infections are often overlooked because low resolution models only reflect a tiny part of the immune system being studied. However, delays are common in the immune system [22]. Often referred to as integer order calculus, fractional calculus (FC) has a history as old as classical calculus. Initially, the FC concept developed gradually. Nonetheless, it has garnered a lot of attention from scholars in recent decades due to its expanding applications in science and engineering. Fractional derivatives are commonly used to explain many materials and processes with memory and hereditary properties [23]. Mathematical models are essential tools for effectively studying the transmission and management of any infectious disease [24]. In many scientific disciplines, fractional calculus is essential, especially in physics and engineering. Because fractional order models distinguish between genetic and memory components of mathematical models, they are more factual and empirical than typical integer order models [25]. A new p-Laplacian non-periodic boundary value issue was studied using extended Caputo fractional derivatives. Different authors utilizes different factional tools under mathematical modeling including stability on different infections phenomena [26–28]. Therefore, in order to prevent and effectively treat bacterial conjunctivitis, it is crucial to understand how it spreads which our extended work under fractional approach. Globally, vaccination campaigns have played a pivotal role in reducing the incidence of infectious diseases [29]. A vaccine effort might significantly curb the development of conjunctivitis, which is spreading throughout Kenya. Mathematical modeling is a helpful technique for investigating the potential impacts of these vaccination efforts on disease transmission patterns. In order to identify the best immunization approaches to stop repeated infections, researchers also looked at how environmental factors contribute to the spread of bacterial conjunctivitis

[30, 31]. The aim of the our work is to investigate conjunctivitis pink infection under stochastic time delay haemorrhagic conjunctivitis disease model.
A few definitions may be found in [32–34].

Definition 1.1:
For fractional order $\pi \in (0,1)$, the Riemann Liouville integral may be expressed as follows if $\mathbb{H}$ is a continuous function on $L^1([0,T],\mathbb{R})$.

$$ {}_0^{RL}I_t^{\pi}\mathbb{H}(t) = \frac{1}{\Gamma(\pi)}\int_0^t (t-\tau_2)^{(\pi-1)}\mathbb{H}(\tau_2)d\tau_2, $$

Where $(0,\infty)$ is the pointwise definition of the integral on the right side.

Definition 1.2:
Let $\mathbb{H}$ be a continuous function with a value of $[0,T]$. Consequently, the Caputo derivative of $\mathbb{H}$ may be expressed as follows:

$$ {}_0^{C}D_t^{\pi}\mathbb{H}(t) = \frac{1}{\Gamma(c-\pi)}\left[\int_0^t (t-\tau_2)^{c-\pi-1}\frac{d^n}{d\tau_2^n}\mathbb{H}(t)(\tau_2)d\tau_2\right], $$

The formula for the Gamma function is $\Gamma(.)$. If $n=1$, the above equation may be written like this:

$$ {}_0^{C}D_t^{\pi}\mathbb{H}(t) = \frac{1}{\Gamma(c-\pi)}\left[\int_0^t (t-\tau_2)^{-\pi}\mathbb{H}'(t)(\tau_2)d\tau_2\right]. $$

Definition 1.3:
The fractional order derivative of Atangana Baleanu in Lioville Captuo ABC (Atangana Balunue Captuo) is as follows:

$$ {}_0^{C}D_t^{\tau_2}\{f(t)\} = \frac{AB(\tau_2)}{c-\tau_2}\int_0^t \frac{d^n}{d\tau_2^c}f(\tau_2)E_{\tau_2}[-\tau_2\frac{(t-\tau_2)^{\tau_2}}{c-\tau_2}]d\tau_2, c-1<\tau_2<c $$

Where $AB(0) = AB(1) = 1$ and E_{τ_2} are the Mittage Lefflar functions. Laplace transform (1) is provided below.

$$ [{}_0^{ABC}D_t^{\tau_2}f(t)](W) = \frac{AB(\tau_2)}{1-\tau_2}\frac{W^{\tau_2}L[f(t)](W) - W^{\tau_2-1}f(0)}{W^{\tau_2}+\frac{r}{r-1}} $$

Lemma 1.1:
A fixed location λ^* is thought to represent the equilibrium point of the Caputo system [35].

$$ {}_0^{C}D_t^{\pi}\mathbb{H}(t) = \mathbb{H}(t,\lambda(t)), \qquad \pi \in (0,1), $$

Only if We see that $\mathbb{H}(t,\lambda^*) = 0$.
Using mathematical models to improve vaccination tactics to lower the incidence of bacterial conjunctivitis in Kenya based on meteorological conditions like temperature and humidity is our aim in this work. Our objective is to create vaccine technology that will stop conjunctivitis from spreading throughout Kenya. We look at mass vaccinations, where all community members get vaccinated, and we set up the conditions and resources

needed to make it possible to deliver vaccines within a set amount of time.
In order to comprehend the innovation, Section 1 includes an introduction and historical context. The mathematical model with Caputo fractional operator is formulated in Section 2 under the developed hypothesis with time delay impact. Equilibrium, reproductive number, and sensitivity analysis are covered in Section 3. Section 4 discusses uniqueness and existence using the Caputo Operator. In Section 5, Caputo fractional operator analysis is used to develop numerical solutions. Section 6 provides a detailed physical interpretation of the simulation that was conducted using MATLAB coding. Section 7 examines the constructed model's chaos control, and Section 8 presents the findings.

2. Stochastic time delay model formulation

A nonlinear model for conjunctivitis illness is presented in this section. As with the pandemic of conjunctivitis, an epidemiological model is advised [36]. The SEIR model is frequently used to investigate the transmission of conjunctivitis. Additional research has improved the SEIR model for conjunctivitis. To prevent the spread of infection due to disease, the novel model $C_sC_eC_vC_iC_r$ is constructed with stochastic features, including time delay. Vaccination strategies are also included. Five compartments are used to classify the population at time t:

Description of Variables

- Conjunctivitis disease susceptibility is represented by $C_s(t)$.
- Conjunctivitis disease exposed individuals is represented by $C_e(t)$.
- Conjunctivitis disease vaccinated individuals is represented by $C_v(t)$.
- Conjunctivitis disease infected individuals is represented by $C_i(t)$.
- Conjunctivitis disease recovered individuals is represented by $C_r(t)$.

Description of Parameters

- β stands for the individuals who are born into or immigrated to the susceptible class.
- The natural death rate is denoted by χ.
- ζ indicates that an infected person will migrate to the exposed class when they come into touch with someone who is susceptible.
- σ is the transfer rate between $C_e(t)$ and $C_v(t)$.
- γ indicates which members of the exposed class join the infected class.
- The death rate from an infected class is denoted by b.
- The members of the vaccinated class who enter the infected class are represented by ν.

- α denotes the number of members of the infected class who join the recovered class.
- The parameter π denotes the proportion of vaccinated individuals who transition into the recovered class.
- $(t-\tau)$ represent the time delay

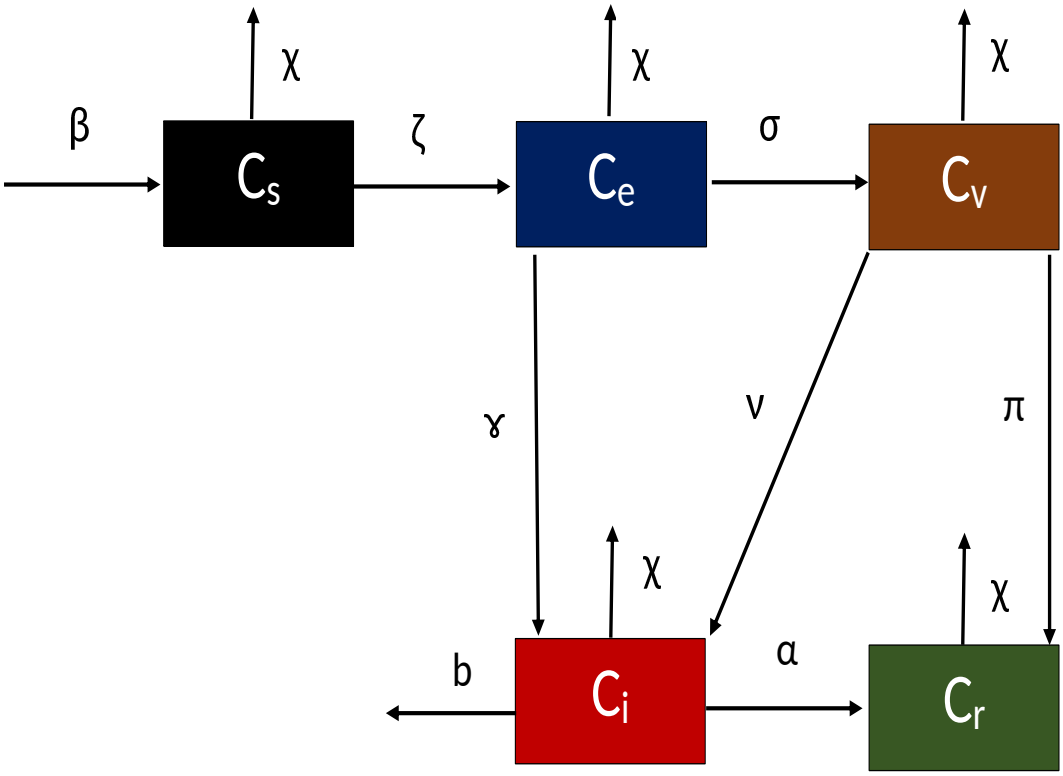

Figure 1: Schematic representation of the newly developed model $C_sC_eC_vC_iC_r$

The mathematical model will be determined by the hypothesis and flow diagram we have built.

$$\begin{cases} \frac{dC_s(t)}{dt} = \beta - \chi C_s(t) - \zeta C_e(t)C_s(t), \\ \frac{dC_e(t)}{dt} = \zeta C_e(t)C_s(t) - (\chi + \sigma + \gamma)C_e(t), \\ \frac{dC_v(t)}{dt}) = \sigma C_e(t) - (\chi + \nu + \pi)C_v(t), \\ \frac{dC_i(t)}{dt} = \gamma C_e(t) + \nu C_v(t) - (\chi + b + \alpha)C_i(t)(t-\tau), \\ \frac{dC_r(t)}{dt} = \pi C_v(t) + \alpha C_i(t)(t-\tau) - \chi C_r(t). \end{cases} \tag{1}$$

The following criteria are all non-negative: $C_s = C_s^0$, $C_e = C_e^0$, $C_v = C_v^0$, $C_i = C_i^0$, and $C_r = C_r^0$. The newly created model, using the Caputo operator, is:

$$\begin{cases} {}^{C}\mathbb{D}_t^{\tau_1} C_s(t) = \beta - \chi C_s(t) - \zeta C_e(t) C_s(t), \\ {}^{C}\mathbb{D}_t^{\tau_1} C_e(t) = \zeta C_e(t) C_s(t) - (\chi + \sigma + \gamma) C_e(t), \\ {}^{C}\mathbb{D}_t^{\tau_1} C_v(t) = \sigma C_e(t) - (\chi + \nu + \pi) C_v(t), \\ {}^{C}\mathbb{D}_t^{\tau_1} C_i(t) = \gamma C_e(t) + \nu C_v(t) - (\chi + b + \alpha) C_i(t)(t - \tau), \\ {}^{C}\mathbb{D}_t^{\tau_1} C_r(t) = \pi C_v(t) + \alpha C_i(t)(t - \tau) - \chi C_r(t). \end{cases} \tag{2}$$

Here ${}^{C}\mathbb{D}_t^{\tau_1}$ is the Caputo and $0 < \tau_1 \leq 1$. Here the conditions $C_s = C_s^0$, $C_e = C_e^0$, $C_v = C_v^0$, $C_i = C_i^0$, $C_r = C_r^0$ are all non-negative.

3. Reproductive numbers, equilibrium points, and sensitivity analysis

The system of equations (2) equals zero in order to determine the equilibrium positions.

$$\beta - \chi C_s(t) - \zeta C_e(t) C_s(t) = 0,$$

$$\zeta C_e(t) C_s(t) - (\chi + \sigma + \gamma) C_e(t) = 0,$$

$$\sigma C_e(t) - (\chi + \nu + \pi) C_v(t) = 0,$$

$$\gamma C_e(t) + \nu C_v(t) - (\chi + b + \alpha) C_i(t)(t - \tau) = 0,$$

$$\pi C_v(t) + \alpha C_i(t)(t - \tau) - \chi C_r(t) = 0.$$

The disease-free equilibrium points of our mathematical model;

$$D_1(C_s, \mathbb{R}) = C_s \to \frac{\beta}{\chi}, C_e \to 0, C_v \to 0, C_i \to 0, C_r \to 0.$$

Where;

$$\mathbb{R} = C_e, C_v, C_i, C_r$$

The endemic equilibrium points are listed below:

$$D_2(C_s,\mathbb{R}) = \begin{cases} C_s^* \to \frac{\gamma+\sigma}{\zeta}, \\ C_e^* \to \frac{\gamma(-\chi)-\chi\sigma+\zeta\beta}{\zeta(\gamma+\sigma)}, \\ C_v^* \to \frac{-\gamma\chi\sigma-\chi\sigma^2+\zeta\beta\sigma}{\zeta(\gamma+\sigma)(\chi+\nu+\pi)}, \\ C_i^* \to -\frac{(\gamma\nu+\gamma\pi+\gamma\chi+\nu\sigma)(\gamma\chi+\chi\sigma-\zeta\beta)}{\zeta(\gamma+\sigma)(\chi+\nu+\pi)(\chi+\alpha+b)}, \\ C_r^* \to -\frac{(\gamma\chi+\chi\sigma-\zeta\beta)(\gamma\nu\alpha+\gamma\pi\alpha+\gamma\chi\alpha+\chi\pi\sigma+\nu\alpha\sigma+\pi\alpha\sigma+\pi b\sigma)}{\chi\zeta(\gamma+\sigma)(\chi+\nu+\pi)(\chi+\alpha+b)}. \end{cases}$$

3.1. Reproductive Number

The Jacobian matrices F and V, which represent the functions F and V, respectively, were understood based on the disease-free level equilibrium point. $\mathbf{R}_0$ is reproduced by obtaining FV^{-1}:

$$J_0 = \begin{pmatrix} -\chi & -\zeta\frac{\beta}{\chi} & 0 & 0 & 0 \\ 0 & \zeta\frac{\beta}{\chi} - (\chi+\sigma+\gamma) & 0 & 0 & 0 \\ 0 & \sigma & -(\chi+\nu+\pi) & 0 & 0 \\ 0 & \gamma & \nu & -(\chi+b+\alpha) & 0 \\ 0 & 0 & \pi & \alpha & -\chi \end{pmatrix}$$

And;

$$J_0 = F - V$$

Where;

$$F = \begin{pmatrix} 0 & 0 & 0 & 0 & 0 \\ 0 & \zeta\frac{\beta}{\chi} & 0 & 0 & 0 \\ 0 & \sigma & 0 & 0 & 0 \\ 0 & \gamma & \nu & 0 & 0 \\ 0 & 0 & \pi & \alpha & 0 \end{pmatrix}$$

$$V = \begin{pmatrix} \chi & \zeta\frac{\beta}{\chi} & 0 & 0 & 0 \\ 0 & \chi+\sigma+\gamma & 0 & 0 & 0 \\ 0 & 0 & \chi+\nu+\pi & 0 & 0 \\ 0 & 0 & 0 & \chi+b+\alpha & 0 \\ 0 & 0 & 0 & 0 & \chi \end{pmatrix}$$

Where;

$$V^{-1}=\begin{pmatrix} \frac{\gamma+\chi+\sigma}{\chi^2+\gamma\chi+\chi\sigma} & -\frac{\zeta\beta}{\chi(\chi^2+\gamma\chi+\chi\sigma)} & 0 & 0 & 0 \\ 0 & \frac{\chi^2+\chi\nu+\chi\pi}{(\chi^2+\gamma\chi+\chi\sigma)(\chi+\nu+\pi)} & 0 & 0 & 0 \\ 0 & 0 & \frac{1}{\chi+\nu+\pi} & 0 & 0 \\ 0 & 0 & 0 & \frac{1}{b+\chi+\alpha} & 0 \\ 0 & 0 & 0 & 0 & \frac{1}{\chi} \end{pmatrix}$$

We can write;

$$K=FV^{-1}$$

Where;

$$K=\begin{pmatrix} 0 & 0 & 0 & 0 & 0 \\ 0 & \frac{\zeta\beta\left(\chi^2+\chi\nu+\chi\pi\right)}{\chi(\chi^2+\gamma\chi+\chi\sigma)(\chi+\nu+\pi)} & 0 & 0 & 0 \\ 0 & \frac{\sigma\left(\chi^2+\chi\nu+\chi\pi\right)}{(\chi^2+\gamma\chi+\chi\sigma)(\chi+\nu+\pi)} & 0 & 0 & 0 \\ 0 & \frac{\gamma\left(\chi^2+\chi\nu+\chi\pi\right)}{(\chi^2+\gamma\chi+\chi\sigma)(\chi+\nu+\pi)} & \frac{\nu}{\chi+\nu+\pi} & 0 & 0 \\ 0 & 0 & \frac{\pi}{\chi+\nu+\pi} & \frac{\alpha}{b+\chi+\alpha} & 0 \end{pmatrix}$$

$$|K-\lambda I|=0$$

$$\begin{vmatrix} 0-\lambda & 0 & 0 & 0 & 0 \\ 0 & \frac{\zeta\beta\left(\chi^2+\chi\nu+\chi\pi\right)}{\chi(\chi^2+\gamma\chi+\chi\sigma)(\chi+\nu+\pi)}-\lambda & 0 & 0 & 0 \\ 0 & \frac{\sigma\left(\chi^2+\chi\nu+\chi\pi\right)}{(\chi^2+\gamma\chi+\chi\sigma)(\chi+\nu+\pi)} & 0-\lambda & 0 & 0 \\ 0 & \frac{\gamma\left(\chi^2+\chi\nu+\chi\pi\right)}{(\chi^2+\gamma\chi+\chi\sigma)(\chi+\nu+\pi)} & \frac{\nu}{\chi+\nu+\pi} & 0-\lambda & 0 \\ 0 & 0 & \frac{\pi}{\chi+\nu+\pi} & \frac{\alpha}{b+\chi+\alpha} & 0-\lambda \end{vmatrix}=0$$

$$\lambda^4\left(\frac{\zeta\beta\left(\chi^2+\chi\nu+\chi\pi\right)}{\chi\left(\chi^2+\gamma\chi+\chi\sigma\right)\left(\chi+\nu+\pi\right)}-\lambda\right)=0$$

Thus, the following values will be found:

$$\lambda\rightarrow\frac{\zeta\beta}{\chi(\gamma+\chi+\sigma)}$$

Our reproductive number is therefore

$$\mathbf{R}_0=\frac{\zeta\beta}{\chi(\gamma+\chi+\sigma)}\ <1$$

$\mathbf{R}_0$ is the average number of infection cases in a susceptible group that are brought on by an infected person in the early or late stages of the illness. The population is not infected while $\mathbf{R}_0$ is less than 1, but it may get infected when $\mathbf{R}_0$ is more than 1.

3.2. The analysis of sensitivity

Sensitivity analysis is used to examine the effects of various factors on the proposed model. The following analytical examples illustrate the effect of each parameter in $\mathbf{R}_0$:

$$\mathbf{R}_0 = \frac{\zeta\beta}{\chi(\gamma+\chi+\sigma)} \ < 1$$

The sensitivity of $\mathbf{R}_0$ can be analyzed by computing the partial derivatives of the threshold value with respect to the corresponding parameters listed below.

$$\begin{cases} \frac{\partial \mathbf{R}_0}{\partial \beta} = \frac{\zeta}{\chi(\gamma+\chi+\sigma)} > 0, \\ \frac{\partial \mathbf{R}_0}{\partial \chi} = -\frac{\zeta\beta}{\chi^2(\gamma+\chi+\sigma)} - \frac{\zeta\beta}{\chi(\gamma+\chi+\sigma)^2} < 0, \\ \frac{\partial \mathbf{R}_0}{\partial \zeta} = \frac{\beta}{\chi(\gamma+\chi+\sigma)} > 0, \\ \frac{\partial \mathbf{R}_0}{\partial \sigma} = -\frac{\zeta\beta}{\chi(\gamma+\chi+\sigma)^2} < 0, \\ \frac{\partial \mathbf{R}_0}{\partial \gamma} = -\frac{\zeta\beta}{\chi(\gamma+\chi+\sigma)^2} < 0. \end{cases}$$

It is evident that $\mathbf{R}_0$ is sensitive when appropriate parametric values are used. We see that while $\beta,\ \zeta$ are increasing, $\chi,\ \sigma,\ \gamma$ are contracting.

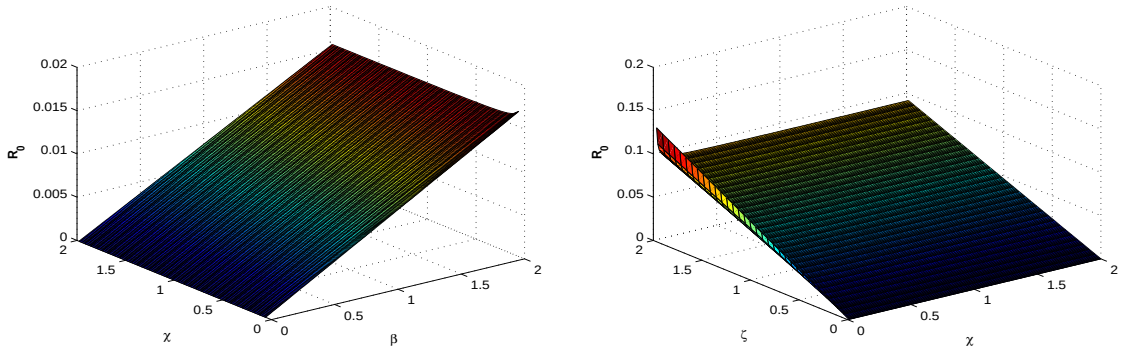

(a) Parameter sensitivity to β and χ (b) Parameter sensitivity to χ and ζ

Figure 2: Sensitivity analysis to several parameters

The variation in the rate of change illustrates that the value of $\mathbf{R}_0$ is highly sensitive, as shown in each subfigure. When the sensitivity index is positive, an increase in the parameter value leads to a rise in $\mathbf{R}_0$. In contrast, a negative sensitivity index implies that $\mathbf{R}_0$ decreases as the parameter value grows. These analytical methods are valuable for identifying the key factors influencing the potential spread of a disease.

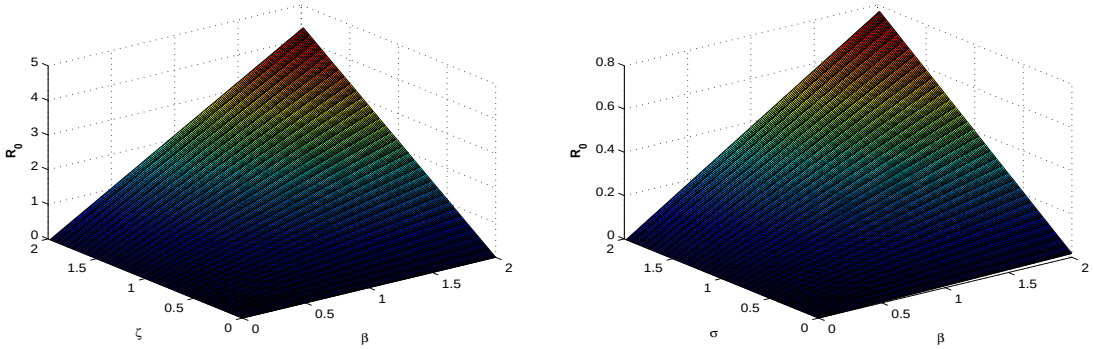

(a) Parameter sensitivity to β and ζ (b) Parameter sensitivity to β and σ

Figure 3: Sensitivity analysis to several parameters

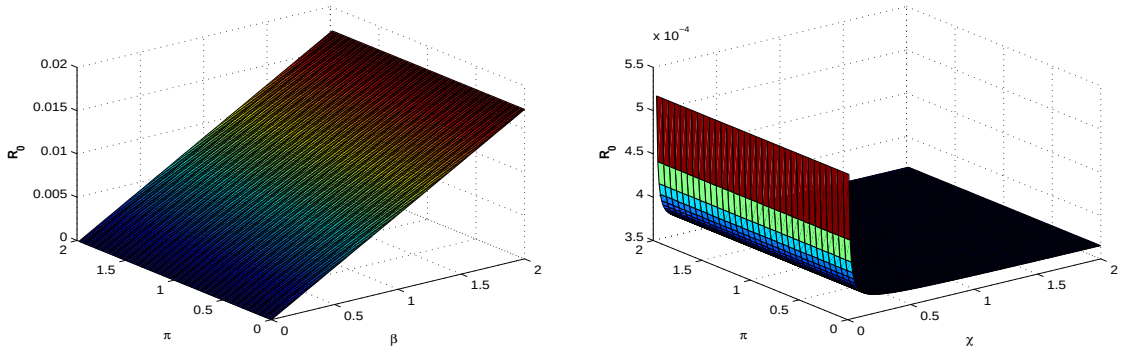

(a) Parameter sensitivity to β and π (b) Parameter sensitivity to χ and π

Figure 4: Sensitivity analysis to several parameters

4. Uniqueness and existence analysis using the Caputo operator

In this section, we used fixed-point theory to investigate the existence and uniqueness of the proposed model. Banach's contraction theorem guarantees the model's singularity, but Schauder's fixed-point theorem guarantees the model's existence. Because they suggest that there is a unique method to address your problem, theorems asserting that our model has a unique solution are important. We can estimate a solution using numerical methods if we are certain that it exists. System (2) may be generalized to a fractional derivative in the Caputo sense for $0 < \tau_1 \leq 1$.

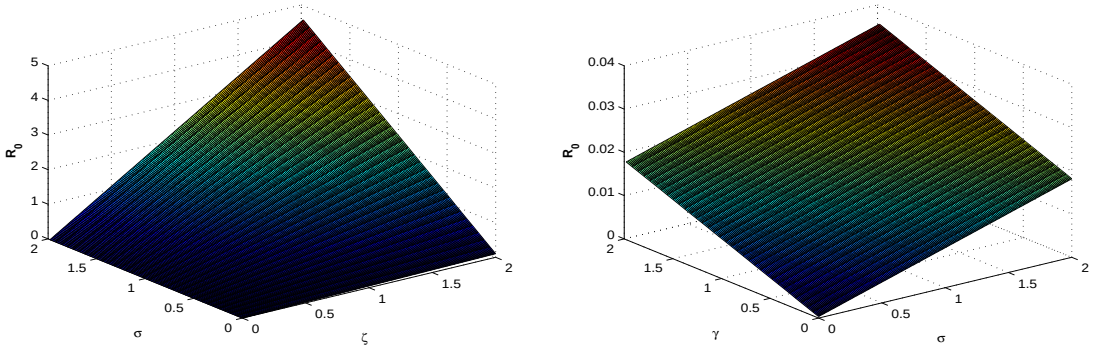

(a) Parameter sensitivity to ζ and σ (b) Parameter sensitivity to σ and γ

Figure 5: Sensitivity analysis to several parameters

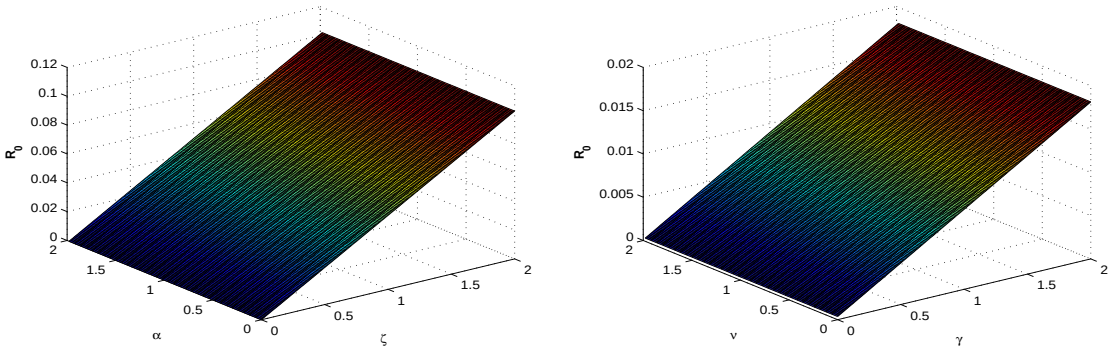

(a) Parameter sensitivity to ζ and α (b) Parameter sensitivity to γ and ν

Figure 6: Sensitivity analysis to several parameters

Let;

$$\begin{cases} \Xi_1(t, C_s) = \beta - \chi C_s(t) - \zeta C_e(t) C_s(t), \\ \Xi_2(t, C_e) = \zeta C_e(t) C_s(t) - (\chi + \sigma + \gamma) C_e(t), \\ \Xi_3(t, C_v) = \sigma C_e(t) - (\chi + \nu + \pi) C_v(t), \\ \Xi_4(t, C_i) = \gamma C_e(t) + \nu C_v(t) - (\chi + b + \alpha) C_i(t)(t - \tau), \\ \Xi_5(t, C_r) = \pi C_v(t) + \alpha C_i(t)(t - \tau) - \chi C_r(t). \end{cases} \tag{3}$$

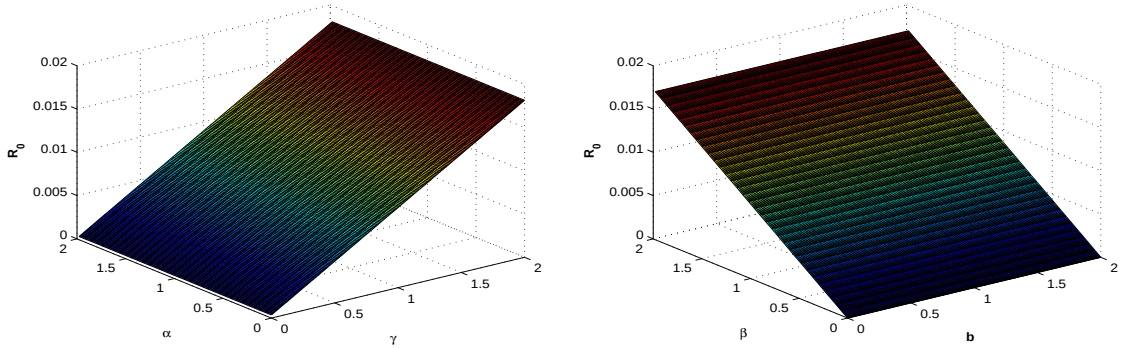

(a) Parameter sensitivity to γ and α (b) Parameter sensitivity to b and β

Figure 7: Sensitivity analysis to several parameters

Using the fractional integral and beginning conditions, we obtain

$$C_s(t) = C_{s_0} + \frac{1}{\Gamma(\tau_1)} \int_0^t (t-\Pi)^{\tau_1 - 1} \Xi_1(t, C_s) d\Pi. \tag{4}$$

Similarly we can find the solution of $C_e(t), C_v(t), C_i(t), C_r(t)$. Let;

$$\Xi(t) = \begin{cases} C_s(t) \\ C_e(t) \\ C_v(t) \\ C_i(t) \\ C_r(t) \end{cases}, \Xi_0 = \begin{cases} C_{s_0} \\ C_{e_0} \\ C_{v_0} \\ C_{i_0} \\ C_{r_0} \end{cases}, \mathbb{Q}(\Pi, \Xi(\Pi) = \begin{cases} \Xi_1(t, C_s), \\ \Xi_2(t, C_e), \\ \Xi_3(t, C_v), \\ \Xi_4(t, C_i), \\ \Xi_5(t, C_r). \end{cases} \tag{5}$$

Thus, system (4) becomes into;

$$\Xi(t) = \Xi_0 + \frac{1}{\Gamma(\tau_1)} \int_0^t (t-\Pi)^{\tau_1 - 1} \mathbb{Q}(\Pi, \Xi(\Pi) d\Pi.$$

Let us now assume a Banach space with a norm $\wp[0, \mathbb{T}] = \nu$:

$$\|C_s, C_e, C_v, C_i, C_r\| = \max_{t \in [0, \mathbb{T}]} [|C_s, C_e, C_v, C_i, C_r|].$$

Let $\mho : \nu \to \nu$ be the definition of a mapping;

$$\mho \Xi(t) = \Xi_0 + \frac{1}{\Gamma(\tau_1)} \int_0^t (t-\Pi)^{\tau_1 - 1} \mathbb{Q}(\Pi, \Xi(\Pi) d\Pi.$$

Next, we apply a nonlinear function to the following assumptions:
P1) There are positive constants ζ_m such that;

$$|\mathbb{Q}(t, \Xi(t)| \leq \zeta_m |\Xi(t)| + \zeta_m. \tag{6}$$

P2) For every $\Xi, \bar{\Xi} \in \nu$, there exists a constant $\tau_m > 0$ such that ;

$$|\mathbb{Q}(t, \bar{\Xi}) - \mathbb{Q}(t, \bar{\Xi}_1)| \leq \tau_m |\bar{\Xi} - \bar{\Xi}_1|. \tag{7}$$

Theorem 4.1: System (2) has a minimum of one solution if $(P1)$ is true.
Proof: Let $\Omega = \{\Xi \in \Omega | \zeta \geq \|\Xi\|\}$ to show that $\mho$ is limited.

$$\zeta \geq \max_{t\in[0,\mathbb{T}]} \frac{\Xi_0 + \left(\frac{\zeta_m \mathbb{T}^{\tau_1}}{\Gamma(\tau_1+1)}\right)}{1 - \left(\frac{\zeta_m \mathbb{T}^{\tau_1}}{\Gamma(\tau_1+1)}\right)}$$

is a closed , convex subset of ν. Now;

$$\begin{aligned}
\|\mho\Xi\| &= \max_{t\in[0,\mathbb{T}]} |\Xi_0 + \frac{1}{\Gamma(\tau_1)} \int_0^t (t-\Pi)^{\tau_1-1} \mathbb{Q}(\Pi, \Xi(\Pi) d\Pi| \\
&\leq |\Xi_0| + \frac{1}{\Gamma(\tau_1)} \int_0^t (t-\Pi)^{\tau_1-1} |\mathbb{Q}(\Pi, \Xi(\Pi)| d\Pi \\
&\leq |\Xi_0| + \frac{1}{\Gamma(\tau_1)} \int_0^t (t-\Pi)^{\tau_1-1} [\zeta_m |\Xi(t)| + \zeta_m] d\Pi \\
&\leq |\Xi_0| + [\zeta_m \|\Xi\| + \zeta_m] \frac{\mathbb{T}^{\tau_1}}{\Gamma(\tau_1+1)} \leq \zeta.
\end{aligned}$$

Since $\Xi \in \Omega \Rightarrow \mho(\Omega) \subseteq \Omega$, it shows that $\mho$ is bounded. Let $t_1 < t_2 \in [0, \mathbb{T}]$, to prove that $\mho$ is completely continuous and take

$$\begin{aligned}
\|\mho\Xi(t_2) - \mho\Xi(t_1)\| &= |\frac{1}{\Gamma(\tau_1)} \int_0^{t_2} (t_2-\Pi)^{\tau_1-1} \mathbb{Q}(\Pi, \Xi(\Pi) d\Pi \\
&- \frac{1}{\Gamma(\tau_1)} \int_0^{t_1} (t_1-\Pi)^{\tau_1-1} \mathbb{Q}(\Pi, \Xi(\Pi) d\Pi| \\
&\leq [\zeta_m \|\Xi\| + \zeta_m] \frac{[t_2^{\tau_1} - t_1^{\tau_1}]}{\Gamma(\tau_1+1)}.
\end{aligned}$$

Accordingly, $t_2 \to t_1$ equals $\|\mho\Xi(t_2) - \mho\Xi(t_1)\| \to 0$. The operator $\mho$ is completely continuous, as demonstrated by the Arzela-Ascoli theorem. Schauder's fixed point theorem states that the given system (2) has at least one solution. The unique solution of system (2) was subsequently demonstrated using the Banach fixed point theorem.
Theorem 4.2: The system (2) is considered to possess a unique solution provided that the conditions $(P2)$ are fulfilled.
Proof: Let $\bar{\Xi}, \bar{\Xi}_1 \in \beta$. Take;

$$\begin{aligned}
\|\mho(\bar{\Xi}) - \mho(\bar{\Xi}_1)\| &= \max_{t\in[0,\mathbb{T}]} |\frac{1}{\Gamma(\tau_1)} \int_0^t (t_2-\Pi)^{\tau_1-1} \mathbb{Q}(\Pi, \bar{\Xi}(\Pi) d\Pi \\
&- \frac{1}{\Gamma(\tau_1)} \int_0^t (t_1-\Pi)^{\tau_1-1} \mathbb{Q}(\Pi, \bar{\Xi}_1(\Pi) d\Pi|
\end{aligned}$$

$$\leq \frac{T^{\tau_1}}{\Gamma(\tau_1+1)}\tau_m|\bar{\Xi}-\bar{\Xi}_1|.$$

Hence, $\mho$ is a contraction. The Banach fixed point theorem indicates that there is only one solution to system (2).

Theorem 4.3: When f, g, h, i, and j are continuous and assumption number two is met, the system has at least one solution if $(\frac{1-\tau_1}{K(\tau_1)})$where $L = max\{L_f, L_g, L_h, L_i, L_j\}$ and $L < 1$

Proof: The fixed point theorem of Krasnosselskii can be used to verify existence results. $\Lambda = (\Lambda_1, \Lambda_2, \Lambda_3, \Lambda_4, \Lambda_5)$ $, \Theta = (\Theta_1, \Theta_2, \Theta_3, \Theta_4, \Theta_5)$ are defined as follows:

$$\begin{cases} \Lambda_1\mathbb{N}(t) = C_{s_0} + \frac{1-\tau_1}{K(\tau_1)}f(t,\mathbb{N}(t)), \\ \Theta_1\mathbb{N}(t) = \frac{\tau_1}{\Gamma(\tau_1)K(\tau_1)}\int_0^t(t-\iota)^{\tau_1-1}f(\iota,\mathbb{N}(\iota))d\iota, \\ \Lambda_2\mathbb{N}(t) = C_{e_0} + \frac{1-\tau_1}{K(\tau_1)}g(t,\mathbb{N}(t)), \\ \Theta_2\mathbb{N}(t) = \frac{\tau_1}{\Gamma(\tau_1)K(\tau_1)}\int_0^t(t-\iota)^{\tau_1-1}g(\iota,\mathbb{N}(\iota))d\iota, \\ \Lambda_3\mathbb{N}(t) = C_{v_0} + \frac{1-\tau_1}{K(\tau_1)}h(t,\mathbb{N}(t)), \\ \Theta_3\mathbb{N}(t) = \frac{\tau_1}{\Gamma(\tau_1)K(\tau_1)}\int_0^t(t-\iota)^{\tau_1-1}h(\iota,\mathbb{N}(\iota))d\iota \\ \Lambda_4\mathbb{N}(t) = C_{i_0} + \frac{1-\tau_1}{K(\tau_1)}i(t,\mathbb{N}(t)), \\ \Theta_4\mathbb{N}(t) = \frac{\tau_1}{\Gamma(\tau_1)K(\tau_1)}\int_0^t(t-\iota)^{\tau_1-1}i(\iota,\mathbb{N}(\iota))d\iota \\ \Lambda_5\mathbb{N}(t) = C_{r_0} + \frac{1-\tau_1}{K(\tau_1)}j(t,\mathbb{N}(t)), \\ \Theta_5\mathbb{N}(t) = \frac{\tau_1}{\Gamma(\tau_1)K(\tau_1)}\int_0^t(t-\iota)^{\tau_1-1}j(\iota,\mathbb{N}(\iota))d\iota. \end{cases}$$

Where as $\mathbb{N}(t) = C_s(t), C_e(t), C_v(t), C_i(t), C_r(t)$ $, \mathbb{N}(y) = C_s(\iota), C_e(\iota), C_v(\iota), C_i(\iota), C_r(\iota)$ and $\mathbb{N} = (C_s, C_e, C_v, C_i, C_r)$. Θ is a continuous operator and Λ is a contraction as a result. Considering any $\mathbb{N}, (\overline{C_s}, \overline{C_e}, \overline{C_v}, \overline{C_i}, \overline{C_r}) \in B$, we obtain:

$$|\Lambda_1(t,\mathbb{N}(t)) - \Lambda_1(\bar{t},\overline{\mathbb{N}(t)})|$$

$$\leq (\frac{1-\tau_1}{K(\tau_1)})L_f[|C_s-\overline{C_s}| + |C_e-\overline{C_e}| + |C_v-\overline{C_v}| + |C_i-\overline{C_i}| + |C_r-\overline{C_r}|],$$

$$\|\Lambda_2(t,\mathbb{N}(t)) - \Lambda_2(\bar{t},\overline{\mathbb{N}(t)})\|$$

Similarly we can find for L_g, L_h, L_i, L_j. Thus;

$$\|\Lambda(t), \mathbb{N}(t) - \Lambda(\bar{t}, \overline{\mathbb{N}(t)})\|$$

$$\leq (\frac{1-\tau_1}{K\tau_1})[\|\mathbb{N} - (\overline{C_s}, \overline{C_e}, \overline{C_v}, \overline{C_i}, \overline{C_r})\|]$$

It demonstrates that Λ is a contraction, and the definition of the closed subset B of $\mathbb{N}$ is For example, $\mathbb{N} = C_s, C_e, C_v, C_i, C_r$. Given any $\mathbb{N} \in B$, we have the following proof that Θ is compact and continuous:

$$\|\Theta_1(\mathbb{N})\| \max_{t\in[0,T]} \frac{\tau_1}{\Gamma(\tau_1)K(\tau_1)} \int_0^t (t-\iota)^{\tau_1-1} f(\iota, \mathbb{N}(\iota))d\iota$$

$$\leq \frac{T^{\tau_1}}{\Gamma(\tau_1)K(\tau_1)}[\mathbb{C}_f\|A\| + \mathbb{B}_f\|A\| + \mathbb{M}_f],$$

$$\|\Theta_2(\mathbb{N})\| \max_{t\in[0,T]} \frac{\tau_1}{\Gamma(\tau_1)K(\tau_1)} \int_0^t (t-\iota)^{\tau_1-1} g(\iota, \mathbb{N}(\iota))d\iota$$

$$\leq \frac{T^{\tau_1}}{\Gamma(\tau_1)K(\tau_1)}[\mathbb{C}_g\|B\| + \mathbb{B}_g\|B\| + \mathbb{M}_g],$$

$$\|\Theta_3(\mathbb{N})\| \max_{t\in[0,T]} \frac{\tau_1}{\Gamma(\tau_1)K(\tau_1)} \int_0^t (t-\iota)^{\tau_1-1} h(\iota, \mathbb{N}(\iota))d\iota$$

$$\leq \frac{T^{\tau_1}}{\Gamma(\tau_1)K(\tau_1)}[\mathbb{C}_h\|C\| + \mathbb{B}_h\|C\| + \mathbb{M}_h],$$

$$\|\Theta_4(\mathbb{N})\| \max_{t\in[0,T]} \frac{\tau_1}{\Gamma(\tau_1)K(\tau_1)} \int_0^t (t-\iota)^{\tau_1-1} i(\iota, \mathbb{N}(\iota))d\iota$$

$$\leq \frac{T^{\tau_1}}{\Gamma(\tau_1)K(\tau_1)}[\mathbb{C}_i\|C\| + \mathbb{B}_i\|C\| + \mathbb{M}_i],$$

$$\|\Theta_5(\mathbb{N})\| \max_{t\in[0,T]} \frac{\tau_1}{\Gamma(\tau_1)K(\tau_1)} \int_0^t (t-\iota)^{\tau_1-1} j(\iota, \mathbb{N}(\iota))d\iota$$

$$\leq \frac{T^{\tau_1}}{\Gamma(\tau_1)K(\tau_1)}[\mathbb{C}_j\|C\| + \mathbb{B}_j\|C\| + \mathbb{M}_j],$$

Thus;

$$\|\Theta(Z)\| \leq T^{\tau_1} \frac{[(\mathbb{C}_1 + \mathbb{B}_1)r + \mathbb{M}_1]}{K(\tau_1)\Gamma(\tau_1)} = \gamma$$

Where; $\mathbb{C}_1 = \mathbb{C}_f + \mathbb{C}_g + \mathbb{C}_h + \mathbb{C}_i + \mathbb{C}_j$, $\mathbb{B}_1 = \mathbb{B}_f + \mathbb{B}_g + \mathbb{B}_h + \mathbb{B}_i + \mathbb{B}_j$, $\mathbb{M}_1 = \mathbb{M}_f + \mathbb{M}_g + \mathbb{M}_h + \mathbb{M}_i + \mathbb{M}_j$. Hence; We shall demonstrate that Λ is equiv continuous after proving that it is bounded. Assuming $t_1 < t_2 \in [0, T]$, take into account

$$|\Theta_1(\mathbb{N})(t_2) - \Theta_1(\mathbb{N})(t_1)| = \frac{\tau_1}{\Gamma(\tau_1)K(\tau_1)} \times | \int_0^{t_2} (t_2 - \iota)^{\tau_1 - 1} f(\iota, \mathbb{N}(\iota)) d\iota$$

$$- \frac{\tau_1}{\Gamma(\tau_1)K(\tau_1)} \times \int_0^{t_1} (t_1 - \iota)^{\tau_1 - 1} f(\iota, \mathbb{N}(\iota)) d\iota|,$$

$$\leq \frac{\tau_1}{\Gamma(\tau_1)K(\tau_1)} [\int_0^{t_2} (t_2 - \iota)^{\tau_1 - 1} - \int_0^{t_1} (t_2 - \iota)^{\tau_1 - 1}]((\mathbb{C}_f + \mathbb{B}_f))r + \mathbb{M}_f d\iota$$

$$\leq \frac{((\mathbb{C}_f + \mathbb{B}_f))r + \mathbb{M}_f}{K(\tau_1)\Gamma(\tau_1)} [t_2^{\tau_1} - t_1^{\tau_1}].$$

$$|\Theta_2(\mathbb{N})(t_2) - \Theta_2(\mathbb{N})(t_1)| \leq \frac{((\mathbb{C}_g + \mathbb{B}_g))r + \mathbb{M}_g}{K(\tau_1)\Gamma(\tau_1)} [t_2^{\tau_1} - t_1^{\tau_1}],$$

$$|\Theta_3(\mathbb{N})(t_2) - \Theta_3(\mathbb{N})(t_1)| \leq \frac{((\mathbb{C}_h + \mathbb{B}_h))r + \mathbb{M}_h}{K(\tau_1)\Gamma(\tau_1)} [t_2^{\tau_1} - t_1^{\tau_1}],$$

$$|\Theta_4(\mathbb{N})(t_2) - \Theta_4(\mathbb{N})(t_1)| \leq \frac{((\mathbb{C}_i + \mathbb{B}_i))r + \mathbb{M}_i}{K(\tau_1)\Gamma(\tau_1)} [t_2^{\tau_1} - t_1^{\tau_1}],$$

$$|\Theta_5(\mathbb{N})(t_2) - \Theta_5(\mathbb{N})(t_1)| \leq \frac{((\mathbb{C}_j + \mathbb{B}_j))r + \mathbb{M}_j}{K(\tau_1)\Gamma(\tau_1)} [t_2^{\tau_1} - t_1^{\tau_1}].$$

$\|\Theta_1(\mathbb{N})(t_2) - \Theta_1(\mathbb{N})(t_1)\| \longrightarrow 0$ as $t_1 \longrightarrow t_2$.Consequently ,$\|\Theta(\mathbb{N})(t_2) - \Theta(\mathbb{N})(t_1)\| \longrightarrow 0$ as $t_1 \longrightarrow t_2$. Thus, it was demonstrated that Θ is an equivalent continuous operator. The Arzel Ascoli theorem has already been used to demonstrate that Θ is a totally continuous operator and that it is uniformly bounded. Θ thus has a unique solution and is rather tiny.

5. Computational evaluation using the fractional operator

To model power-law behaviors observed in real-world phenomena, the Caputo derivative-formulated with a power-law kernel is widely recommended in the literature. A numerical integration method based on Newton polynomial interpolation is employed to account for the power-law effect inherent in fractional calculus, replacing the standard time derivative with the Caputo form. For problem (2), we present a numerical scheme that utilizes a Newton polynomial for simplification and computational efficiency.

$$\begin{cases} {}^{C}\mathbb{D}_t^{\tau_1} C_s = C_{s_1}(t, C_s), \\ {}^{C}\mathbb{D}_t^{\tau_1} C_e = C_{e_1}(t, C_e), \\ {}^{C}\mathbb{D}_t^{\tau_1} C_v = C_{v_1}(t, C_v), \\ {}^{C}\mathbb{D}_t^{\tau_1} C_i = C_{i_1}(t, C_i), \\ {}^{C}\mathbb{D}_t^{\tau_1} C_r = C_{r_1}(t, C_r). \end{cases} \tag{8}$$

Where;

$$\begin{cases} C_{s_1}(t, C_s) = \beta - \chi C_s(t) - \zeta C_e(t) C_s(t), \\ C_{e_1}(t, C_e) = \zeta C_e(t) C_s(t) - (\chi + \sigma + \gamma) C_e(t), \\ C_{v_1}(t, C_v) = \sigma C_e(t) - (\chi + \nu + \pi) C_v(t), \\ C_{i_1}(t, C_i) = \gamma C_e(t) + \nu C_v(t) - (\chi + b + \alpha) C_i(t)(t - \tau), \\ C_{r_1}(t, C_r) = \pi C_v(t) + \alpha C_i(t)(t - \tau) - \chi C_r(t). \end{cases} \tag{9}$$

With a power law kernel and a fractional integral, we may obtain

$$C_s(t_\upsilon + 1) = C_s(0) + \frac{1}{\Gamma(\tau_1)} \sum_{\xi=2}^{\upsilon} \int_{t_\xi}^{t_{\xi+1}} C_{s_1}(t, C_s) \Psi_1^{1-\Xi} (t_{\upsilon+1} - \Psi_1)^{\tau_1 - 1} d\Psi_1. \tag{10}$$

$$C_e(t_\upsilon + 1) = C_e(0) + \frac{1}{\Gamma(\tau_1)} \sum_{\xi=2}^{\upsilon} \int_{t_\xi}^{t_{\xi+1}} C_{e_1}(t, C_e) \Psi_1^{1-\Xi} (t_{\upsilon+1} - \Psi_1)^{\tau_1 - 1} d\Psi_1. \tag{11}$$

$$C_v(t_\upsilon + 1) = C_v(0) + \frac{1}{\Gamma(\tau_1)} \sum_{\xi=2}^{\upsilon} \int_{t_\xi}^{t_{\xi+1}} C_{v_1}(t, C_v) \Psi_1^{1-\Xi} (t_{\upsilon+1} - \Psi_1)^{\tau_1 - 1} d\Psi_1. \tag{12}$$

$$C_i(t_\upsilon+1) = C_i(0)+\frac{1}{\Gamma(\tau_1)}\sum_{\xi=2}^{\upsilon}\int_{t_\xi}^{t_{\xi+1}} C_{i_1}(t,C_i)\Psi_1^{1-\Xi}(t_{\upsilon+1}-\Psi_1)^{\tau_1-1}d\Psi_1. \quad (13)$$

$$C_r(t_\upsilon+1) = C_r(0)+\frac{1}{\Gamma(\tau_1)}\sum_{\xi=2}^{\upsilon}\int_{t_\xi}^{t_{\xi+1}} C_{r_1}(t,C_r)\Psi_1^{1-\Xi}(t_{\upsilon+1}-\Psi_1)^{\tau_1-1}d\Psi_1. \quad (14)$$

Equations (10) through (14) with the Newton Polynomial substituted:

$$\begin{aligned} C_s(t_\upsilon+1) &= C_s(0)+\frac{1}{\Gamma(\tau_1)}\sum_{\xi=2}^{\upsilon} C_{s_1}(t_{\xi-2},C_s^{\xi-2})t_{\xi-2}^{1-\Xi}\int_{t_\xi}^{t_{\xi+1}}(t_{\upsilon+1}-\Psi_1)^{\tau_1-1}d\Psi_1 \\ &+ \frac{1}{\Gamma(\tau_1)}\sum_{\xi=2}^{\upsilon}\frac{1}{\gamma t}\{t_{\xi-1}^{1-\Xi}C_{s_1}(t_{\xi-1},C_s^{\xi-1})-t_{\xi-2}^{1-\Xi}C_{s_1}(t_{\xi-2},C_s^{\xi-2})\} \\ &\quad \int_{t_\xi}^{t_{\xi+1}}(\Psi_1-t_{\xi-2})(t_{\upsilon+1}-\Psi_1)^{\tau_1-1}d\Psi_1 \\ &+ \frac{1}{\Gamma(\tau_1)}\sum_{\xi=2}^{\upsilon}\frac{1}{2\gamma t^2}\{t_\xi^{1-\Xi}C_{s_1}(t_\xi,C_s^{\xi})-2t_{\xi-1}^{1-\Xi}C_{s_1}(t_{\xi-1},C_s^{\xi-1}) \\ &+ t_{\xi-2}^{1-\Xi}C_{s_1}(t_{\xi-2},C_s^{\xi-2})\}\int_{t_\xi}^{t_{\xi+1}}(\Psi_1-t_{\xi-2})(\Psi_1-t_{\xi-1})(t_{\upsilon+1}-\Psi_1)^{\tau_1-1}d\Psi_1. \end{aligned} \quad (15)$$

$$\begin{aligned} C_e(t_\upsilon+1) &= C_e(0)+\frac{1}{\Gamma(\tau_1)}\sum_{\xi=2}^{\upsilon} C_{e_1}(t_{\xi-2},C_e^{\xi-2})t_{\xi-2}^{1-\Xi}\int_{t_\xi}^{t_{\xi+1}}(t_{\upsilon+1}-\Psi_1)^{\tau_1-1}d\Psi_1 \\ &+ \frac{1}{\Gamma(\tau_1)}\sum_{\xi=2}^{\upsilon}\frac{1}{\gamma t}\{t_{\xi-1}^{1-\Xi}C_{e_1}(t_{\xi-1},C_e^{\xi-1})-t_{\xi-2}^{1-\Xi}C_{e_1}(t_{\xi-2},C_e^{\xi-2})\} \\ &\quad \int_{t_\xi}^{t_{\xi+1}}(\Psi_1-t_{\xi-2})(t_{\upsilon+1}-\Psi_1)^{\tau_1-1}d\Psi_1 \\ &+ \frac{1}{\Gamma(\tau_1)}\sum_{\xi=2}^{\upsilon}\frac{1}{2\gamma t^2}\{t_\xi^{1-\Xi}C_{e_1}(t_\xi,C_e^{\xi})-2t_{\xi-1}^{1-\Xi}C_{e_1}(t_{\xi-1},C_e^{\xi-1}) \\ &+ t_{\xi-2}^{1-\Xi}C_{e_1}(t_{\xi-2},C_e^{\xi-2})\}\int_{t_\xi}^{t_{\xi+1}}(\Psi_1-t_{\xi-2})(\Psi_1-t_{\xi-1})(t_{\upsilon+1}-\Psi_1)^{\tau_1-1}d\Psi_1. \end{aligned} \quad (16)$$

$$C_v(t_\upsilon+1) = C_v(0)+\frac{1}{\Gamma(\tau_1)}\sum_{\xi=2}^{\upsilon} C_{v_1}(t_{\xi-2},C_v^{\xi-2})t_{\xi-2}^{1-\Xi}\int_{t_\xi}^{t_{\xi+1}}(t_{\upsilon+1}-\Psi_1)^{\tau_1-1}d\Psi_1$$

$$
\begin{aligned}
&+ \frac{1}{\Gamma(\tau_1)}\sum_{\xi=2}^{\upsilon}\frac{1}{\gamma t}\{t_{\xi-1}^{1-\Xi}C_{v_1}(t_{\xi-1},C_v^{\xi-1},) - t_{\xi-2}^{1-\Xi}C_{v_1}(t_{\xi-2},C_v^{\xi-2})\}\\
&\int_{t_\xi}^{t_{\xi+1}}(\Psi_1-t_{\xi-2})(t_{\upsilon+1}-\Psi_1)^{\tau_1-1}d\Psi_1\\
&+ \frac{1}{\Gamma(\tau_1)}\sum_{\xi=2}^{\upsilon}\frac{1}{2\gamma t^2}\{t_{\xi}^{1-\Xi}C_{v_1}(t_{\xi},C_v^{\xi}) - 2t_{\xi-1}^{1-\Xi}C_{v_1}(t_{\xi-1},C_v^{\xi-1})\\
&+ t_{\xi-2}^{1-\Xi}C_{v_1}(t_{\xi-2},C_v^{\xi-2},)\}\int_{t_\xi}^{t_{\xi+1}}(\Psi_1-t_{\xi-2})(\Psi_1-t_{\xi-1})(t_{\upsilon+1}-\Psi_1)^{\tau_1-1}d\Psi_1.
\end{aligned}
\tag{17}
$$

$$
\begin{aligned}
C_i(t_\upsilon+1) &= C_i(0)+\frac{1}{\Gamma(\tau_1)}\sum_{\xi=2}^{\upsilon}C_{i_1}(t_{\xi-2},C_i^{\xi-2})t_{\xi-2}^{1-\Xi}\int_{t_\xi}^{t_{\xi+1}}(t_{\upsilon+1}-\Psi_1)^{\tau_1-1}d\Psi_1\\
&+ \frac{1}{\Gamma(\tau_1)}\sum_{\xi=2}^{\upsilon}\frac{1}{\gamma t}\{t_{\xi-1}^{1-\Xi}C_{i_1}(t_{\xi-1},C_i^{\xi-1},) - t_{\xi-2}^{1-\Xi}C_{i_1}(t_{\xi-2},C_i^{\xi-2})\}\\
&\int_{t_\xi}^{t_{\xi+1}}(\Psi_1-t_{\xi-2})(t_{\upsilon+1}-\Psi_1)^{\tau_1-1}d\Psi_1\\
&+ \frac{1}{\Gamma(\tau_1)}\sum_{\xi=2}^{\upsilon}\frac{1}{2\gamma t^2}\{t_{\xi}^{1-\Xi}C_{i_1}(t_{\xi},C_i^{\xi}) - 2t_{\xi-1}^{1-\Xi}C_{i_1}(t_{\xi-1},C_i^{\xi-1})\\
&+ t_{\xi-2}^{1-\Xi}C_{i_1}(t_{\xi-2},C_i^{\xi-2},)\}\int_{t_\xi}^{t_{\xi+1}}(\Psi_1-t_{\xi-2})(\Psi_1-t_{\xi-1})(t_{\upsilon+1}-\Psi_1)^{\tau_1-1}d\Psi_1.
\end{aligned}
\tag{18}
$$

$$
\begin{aligned}
C_r(t_\upsilon+1) &= C_r(0)+\frac{1}{\Gamma(\tau_1)}\sum_{\xi=2}^{\upsilon}C_{r_1}(t_{\xi-2}C_r^{\xi-2})t_{\xi-2}^{1-\Xi}\int_{t_\xi}^{t_{\xi+1}}(t_{\upsilon+1}-\Psi_1)^{\tau_1-1}d\Psi_1\\
&+ \frac{1}{\Gamma(\tau_1)}\sum_{\xi=2}^{\upsilon}\frac{1}{\gamma t}\{t_{\xi-1}^{1-\Xi}C_{r_1}(t_{\xi-1},C_r^{\xi-1}) - t_{\xi-2}^{1-\Xi}C_{r_1}(t_{\xi-2},C_r^{\xi-2})\}\\
&\int_{t_\xi}^{t_{\xi+1}}(\xi-t_{\xi-2})(t_{\upsilon+1}-\Psi_1)^{\tau_1-1}d\Psi_1\\
&+ \frac{1}{\Gamma(\tau_1)}\sum_{\xi=2}^{\upsilon}\frac{1}{2\gamma t^2}\{t_{\xi}^{1-\Xi}C_{r_1}(t_{\xi},C_r^{\xi}) - 2t_{\xi-1}^{1-\Xi}C_{r_1}(t_{\xi-1},C_r^{\xi-1})\\
&+ t_{\xi-2}^{1-\Xi}C_{r_1}(t_{\xi-2},C_r^{\xi-2})\}\int_{t_\xi}^{t_{\xi+1}}(\Psi_1-t_{\xi-2})(\Psi_1-t_{\xi-1})(t_{\upsilon+1}-\Psi_1)^{\tau_1-1}d\Psi_1.
\end{aligned}
$$

(19)

An explanation of how integral computation works in equations (15) – (19) is as:

$$\int_{t_\xi}^{t_{\xi+1}} (t_{\upsilon+1} - \Psi_1)^{\tau_1-1} d\Psi_1 = \frac{(\gamma t)^{\tau_1}}{\tau_1} \left((\upsilon - \xi + 1)^{\tau_1} - (\upsilon - \xi)^{\tau_1} \right).$$

$$\begin{aligned}\int_{t_\xi}^{t_{\xi+1}} (\Psi_1 - t_{\xi-2})(t_{\upsilon+1} - \Psi_1)^{\tau_1-1} d\Psi_1 &= \frac{(\gamma t)^{\tau_1+1}}{\tau_1(\tau_1+1)} \{(\upsilon - \xi + 1)^{\tau_1}(\upsilon - \xi + 3 + 2\tau_1) \\ &- (\upsilon - \xi)^{\tau_1}(\upsilon - \xi + 3 + 3\tau_1)\}.\end{aligned}$$

$$\begin{aligned}\int_{t_\xi}^{t_{\xi+1}} (\Psi_1 - t_{\xi-2})(\Psi_1 - t_{\xi-1})(t_{\upsilon+1} - \Psi_1)^{\tau_1-1} d\Psi_1 &= \frac{(\gamma t)^{\tau_1+2}}{\tau_1(\tau_1+1)(\tau_1+2)} \{(\upsilon - \xi + 1)^{\tau_1}(2(\upsilon - \xi)^2 \\ &+ (3\tau_1 + 10)(\upsilon - \xi) + 2\tau_1^2 + 9\tau_1 + 12) - (\upsilon - \xi)^{\tau_1} \\ &\times (2(\upsilon - \xi)^2 + (5\tau_1 + 10)(\upsilon - \xi) + 6\tau_1^2 + 18\tau_1 + 12)\}.\end{aligned}$$

Finally,we obtain;

$$\begin{aligned}C_s(t_\upsilon + 1) &= C_s(0) + \frac{(\gamma t)^{\tau_1}}{\Gamma(\tau_1+1)} \sum_{\xi=2}^{\upsilon} t_{\xi-2}^{1-\Xi} C_{s_1}(t_{\xi-2}, C_s^{\xi-2}) K_1 \\ &+ \frac{(\gamma t)^{\tau_1}}{\Gamma(\tau_1+2)} \sum_{\xi=2}^{\upsilon} \{t_{\xi-1}^{1-\Xi} C_{s_1}(t_{\xi-1}, C_s^{\xi-1}) - t_{\xi-2}^{1-\Xi} C_{s_1}(t_{\xi-2}, C_s^{\xi-2})\} K_2 \\ &+ \frac{(\gamma t)^{\tau_1}}{\Gamma(\tau_1+3)} \sum_{\xi=2}^{\upsilon} \{t_{\xi}^{1-\Xi} C_{s_1}(t_{\xi}, C_s^{\xi}) - 2t_{\xi-1}^{1-\Xi} C_{s_1}(t_{\xi-1}, C_s^{\xi-1}) + t_{\xi-2}^{1-\Xi} C_{s_1}(t_{\xi-2}, C_s^{\xi-2})\} K_3.\end{aligned}$$

$$\begin{aligned}C_e(t_\upsilon + 1) &= C_e(0) + \frac{(\gamma t)^{\tau_1}}{\Gamma(\tau_1+1)} \sum_{\xi=2}^{\upsilon} t_{\xi-2}^{1-\Xi} C_{e_1}(t_{\xi-2}, C_e^{\xi-2}) K_1 \\ &+ \frac{(\gamma t)^{\tau_1}}{\Gamma(\tau_1+2)} \sum_{\xi=2}^{\upsilon} \{t_{\xi-1}^{1-\Xi} C_{e_1}(t_{\xi-1}, C_e^{\xi-1}) - t_{\xi-2}^{1-\Xi} C_{e_1}(t_{\xi-2}, C_e^{\xi-2})\} K_2 \\ &+ \frac{(\gamma t)^{\tau_1}}{\Gamma(\tau_1+3)} \sum_{\xi=2}^{\upsilon} \{t_{\xi}^{1-\Xi} C_{e_1}(t_{\xi}, C_e^{\xi}) - 2t_{\xi-1}^{1-\Xi} C_{e_1}(t_{\xi-1}, C_e^{\xi-1}) + t_{\xi-2}^{1-\Xi} C_{e_1}(t_{\xi-2}, C_e^{\xi-2})\} K_3.\end{aligned}$$

$$\begin{aligned}C_v(t_\upsilon + 1) &= C_v(0) + \frac{(\gamma t)^{\tau_1}}{\Gamma(\tau_1+1)} \sum_{\xi=2}^{\upsilon} t_{\xi-2}^{1-\Xi} C_{v_1}(t_{\xi-2}, C_v^{\xi-2}) K_1 \\ &+ \frac{(\gamma t)^{\tau_1}}{\Gamma(\tau_1+2)} \sum_{\xi=2}^{\upsilon} \{t_{\xi-1}^{1-\Xi} C_{v_1}(t_{\xi-1}, C_v^{\xi-1}) - t_{\xi-2}^{1-\Xi} C_{v_1}(t_{\xi-2}, C_v^{\xi-2})\} K_2\end{aligned}$$

$$+ \quad \frac{(\gamma t)^{\tau_1}}{\Gamma(\tau_1+3)}\sum_{\xi=2}^{\upsilon}\{t_{\xi}^{1-\Xi}C_{v_1}(t_{\xi},C_v^{\xi}) - 2t_{\xi-1}^{1-\Xi}C_{v_1}(t_{\xi-1},C_v^{\xi-1}) + t_{\xi-2}^{1-\Xi}C_{v_1}(t_{\xi-2},C_v^{\xi-2})\}K_3.$$

$$\begin{aligned}
C_i(t_\upsilon+1) &= C_i(0) + \frac{(\gamma t)^{\tau_1}}{\Gamma(\tau_1+1)}\sum_{\xi=2}^{\upsilon} t_{\xi-2}^{1-\Xi}C_{i_1}(t_{\xi-2},C_i^{\xi-2})K_1 \\
&+ \frac{(\gamma t)^{\tau_1}}{\Gamma(\tau_1+2)}\sum_{\xi=2}^{\upsilon}\{t_{\xi-1}^{1-\Xi}C_{i_1}(t_{\xi-1},C_i^{\xi-1}) - t_{\xi-2}^{1-\Xi}C_{i_1}(t_{\xi-2},C_i^{\xi-2})\}K_2 \\
&+ \frac{(\gamma t)^{\tau_1}}{\Gamma(\tau_1+3)}\sum_{\xi=2}^{\upsilon}\{t_{\xi}^{1-\Xi}C_{i_1}(t_{\xi},C_i^{\xi}) - 2t_{\xi-1}^{1-\Xi}C_{i_1}(t_{\xi-1},C_i^{\xi-1}) + t_{\xi-2}^{1-\Xi}T_1(t_{\xi-2},C_i^{\xi-2})\}K_3.
\end{aligned}$$

$$\begin{aligned}
C_r(t_\upsilon+1) &= C_r(0) + \frac{(\gamma t)^{\tau_1}}{\Gamma(\tau_1+1)}\sum_{\xi=2}^{\upsilon} t_{\xi-2}^{1-\Xi}C_{r_1}(t_{\xi-2},C_r^{\xi-2})K_1 \\
&+ \frac{(\gamma t)^{\tau_1}}{\Gamma(\tau_1+2)}\sum_{\xi=2}^{\upsilon}\{t_{\xi-1}^{1-\Xi}C_{r_1}(t_{\xi-1},C_r^{\xi-1}) - t_{\xi-2}^{1-\Xi}C_{r_1}(t_{\xi-2},C_r^{\xi-2})\}K_2 \\
&+ \frac{(\gamma t)^{\tau_1}}{\Gamma(\tau_1+3)}\sum_{\xi=2}^{\upsilon}\{t_{\xi}^{1-\Xi}C_{r_1}(t_{\xi},C_r^{\xi}) - 2t_{\xi-1}^{1-\Xi}C_{r_1}(t_{\xi-1},C_r^{\xi-1}) + t_{\xi-2}^{1-\Xi}C_{r_1}(t_{\xi-2},C_r^{\xi-2})\}K_3.
\end{aligned}$$

Where;

$$K_1 = (\upsilon-\xi+1)^{\tau_1} - (\upsilon-\xi)^{\tau_1}.$$

$$K_2 = (\upsilon-\xi+1)^{\tau_1}(\upsilon-\xi+3+2\tau_1) - (\upsilon-\xi)^{\tau_1}(\upsilon-\xi+3+3\tau_1).$$

$$\begin{aligned}
K_3 = \quad & (\upsilon-\xi+1)^{\tau_1}(2(\upsilon-\xi)^2 + (3\tau_1+10)(\upsilon-\xi) + 2\tau_1^2 + 9\tau_1 + 12) - (\upsilon-\xi)^{\tau_1}(2(\upsilon-\xi)^2 \\
& + (5\tau_1+10)(\upsilon-\xi) + 6\tau_1^2 + 18\tau_1 + 12).
\end{aligned}$$

6. Physical interpretations

In this case, we developed theoretical conclusions and used an advanced method to evaluate their efficacy. A simulation was used to study the recently constructed system. $\beta = 0.00365$, $\chi = 0.04$, $\zeta = 0.00784$, $\sigma = 0.002$, $\nu = 0.55$, $\pi = 0.855$, $\gamma = 0.04$, $b = 0.33$, $\alpha = 0.276$, $C_s = 0.6$, $C_e = 4.5$, $C_v = 3.5$, $C_i = 1.7$, $C_r = 4.5$ are the initial values for the developed models. Significant findings were obtained using the conjunctivitis model with non-integer (fractional) parameters. Once the fractional orders were reduced to suitable levels, the corresponding model solutions were illustrated in Figures 8 through 12. The following discussion summarizes the numerical simulations of the proposed conjunctivitis

model, performed in MATLAB to confirm the validity of the theoretical results. Figures 8, 11, and 12 illustrate the variations in the susceptible, infected, and recovered populations, respectively. As the fractional orders decrease, these compartments show gradual increases, yielding early and reliable outcomes. Figures 9 and 10 present the behavior of the exposed and vaccinated groups at different fractional orders. Over time, all subcompartments exhibit a sharp decline before stabilizing. The model effectively predicts future infection trends and suggests improved strategies for controlling the spread of conjunctivitis. Employing an advanced computational approach, the study produces accurate and consistent solutions for all compartments at fractional-order derivatives. The reliability of the results strengthens as fractional values decrease. The data further indicate that vaccination significantly boosts immunity among individuals with lower resistance levels, leading to a marked reduction in infections and a corresponding increase in recoveries.

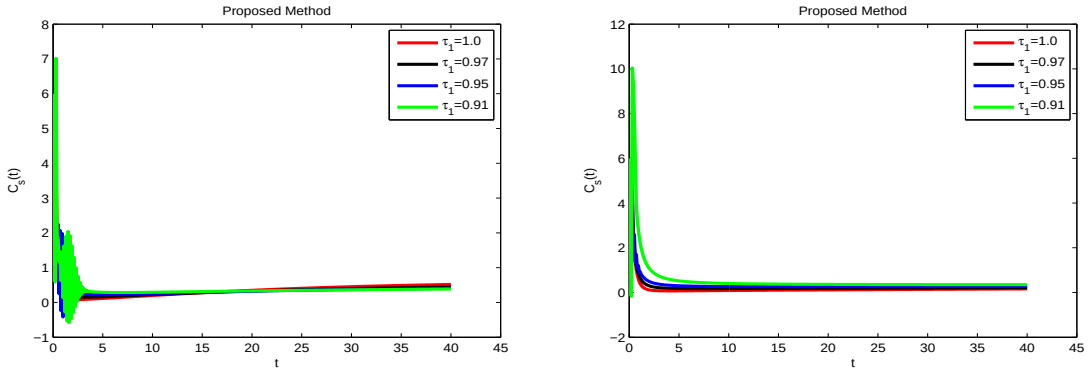

(a) As a dimension, 0.7 (b) As a dimension, 0.4

Figure 8: Making use of the fractal fractional operator, $C_s(t)$

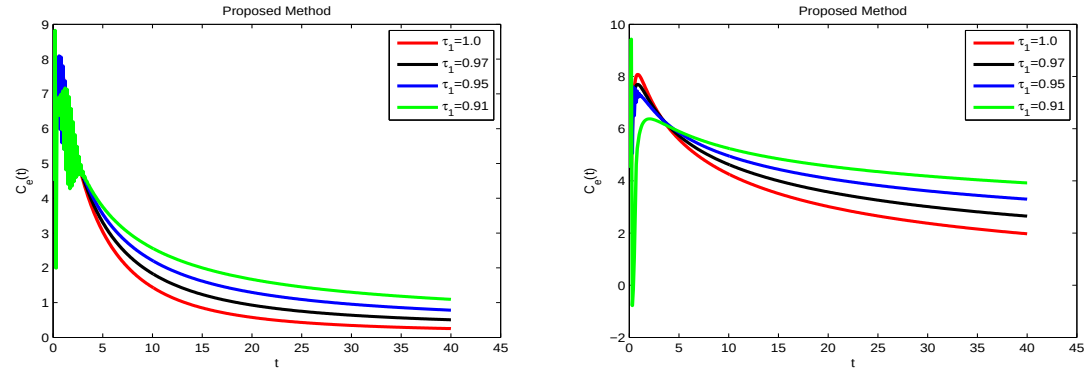

(a) As a dimension, 0.7 (b) As a dimension, 0.4

Figure 9: Making use of the fractal fractional operator, $C_e(t)$

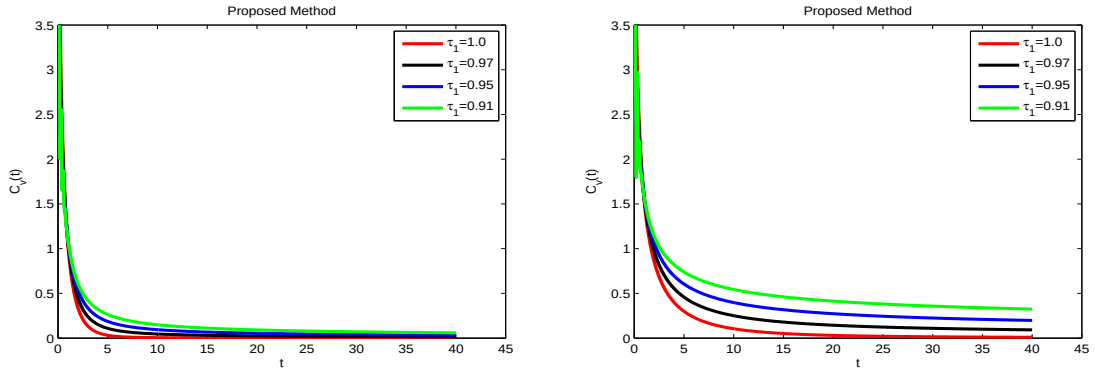

(a) As a dimension, 0.7 (b) As a dimension, 0.4

Figure 10: Making use of the fractal fractional operator, $C_v(t)$

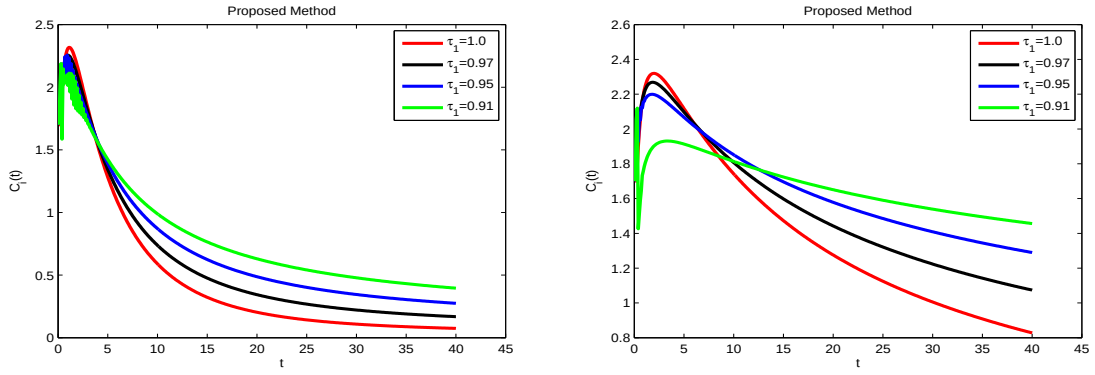

(a) As a dimension, 0.7 (b) As a dimension, 0.4

Figure 11: Making use of the fractal fractional operator, $C_i(t)$

7. Chaos control

Based on its points of equilibrium, it employs the linear feedback regulate approach to stabilize system (2), taking into account a fractional-order system with a regulated design.

$$\begin{cases} {}^{C}\mathbb{D}_t^{\tau_1} C_s(t) = \beta - \chi C_s(t) - \zeta C_e(t) C_s(t) - \gamma_1 (C_s - C_s^*), \\ {}^{C}\mathbb{D}_t^{\tau_1} C_e(t) = \zeta C_e(t) C_s(t) - (\chi + \sigma + \gamma) C_e(t) - \gamma_2 (C_e - C_e^*), \\ {}^{C}\mathbb{D}_t^{\tau_1} C_v(t) = \sigma C_e(t) - (\chi + \nu + \pi) C_v(t) - \gamma_3 (C_v - C_v^*), \\ {}^{C}\mathbb{D}_t^{\tau_1} C_i(t) = \gamma C_e(t) + \nu C_v(t) - (\chi + b + \alpha) C_i(t)(t - \tau) - \gamma_4 (C_i - C_i^*), \\ {}^{C}\mathbb{D}_t^{\tau_1} C_r(t) = \pi C_v(t) + \alpha C_i(t)(t - \tau) - \chi C_r(t) - \gamma_5 (C_r - C_r^*). \end{cases}$$

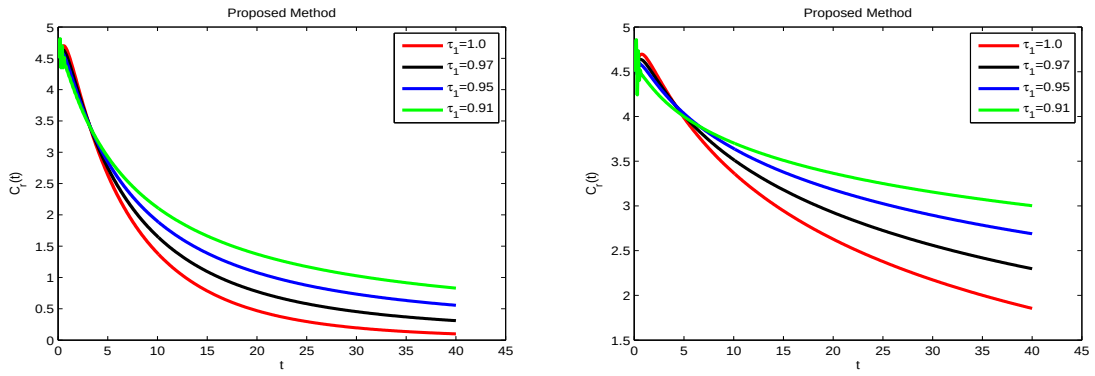

(a) As a dimension, 0.7 (b) As a dimension, 0.4

Figure 12: Making use of the fractal fractional operator, $C_r(t)$

$C_s^*, C_e^*, C_v^*, C_i^*, and C_r^*$ show the system's point of equilibrium, whereas γ_1, γ_2, γ_3, γ_4, and γ_5 represent the control parameters. The following is the Jacobian matrix associated with $\mathbf{D}^*$:

$$\begin{bmatrix} -g-\zeta C_e & -\zeta C_s & 0 & 0 & 0 \\ \zeta C_e & \zeta C_s-(\chi+\sigma+\gamma) & 0 & 0 & 0 \\ 0 & \sigma & -(\chi+\nu+\pi) & 0 & 0 \\ 0 & \gamma & \nu & -(\chi+b+\alpha) & 0 \\ 0 & 0 & \pi & \alpha & -\chi \end{bmatrix}$$

Assuming $\gamma_1 = 1$, $\gamma_2 = 2$, $\gamma_3 = 3$, $\gamma_4 = 4$, and $\gamma_5 = 5$, and with the following parameters: $\beta = 0.003, \chi = 0.004, \zeta = 0.0068, \sigma = 0.007, \nu = 0.04, \pi = 0.0677, \gamma = 0.0099, b = 0.77$, and $\alpha = 0.34$, then

$$C(\lambda) = -\lambda^5 - 0.6753\lambda^4 - 0.77830\lambda^3 - 0.00098\lambda^2 - 0.07654\lambda - 0.000987644 = 0,$$

And;

$$\lambda = -0.538, \quad \lambda = -0.3456, \quad \lambda = -0.098798, \quad \lambda = -0.008, \quad \lambda = -0.0087 \tag{20}$$

Given the parameters $\beta = 0.03, \chi = 0.08, \zeta = 0.056, \sigma = 0.0234, \nu = 0.088, \pi = 0.0579, \gamma = 0.001, b = 0.234$, and $\alpha = 0.0456$. And$\gamma_1 = 1$, $\gamma_2 = 2$, $\gamma_3 = 3$, $\gamma_4 = 4$, and $\gamma_5 = 5$:

$$C(\lambda) = -\lambda^5 - 0.4567\lambda^4 - 0.089087\lambda^3 - 0.0345678\lambda^2 - 0.00234576\lambda = 0,$$

And;

$$\lambda = -0.0999, \quad \lambda = -0.728, \quad \lambda = -0.008, \quad \lambda = -0.004, \quad \lambda = -0.0056 \tag{21}$$

Equations (20) and (21) have asymptotically stable D_1, D_2 since each eigenvalue is negative. The accompanying image displays a simulation of the intended system using various parameter values and fractional order values. Here, we can see that the solutions have a greater effect at a lower minimum interest rate and are limited in the feasible domain.

References

[1] S. A. Ali, S. Ali, I. Jahan, and S. Ali. Allergies to infections: understanding the spectrum of conjunctivitis. *International Journal of Pharmaceutical Drug Design (ijpdd)*, 1(1):46–56, 2023.

[2] C. N. Muli and A. M. Kimulu. Optimizing vaccination strategies to reduce conjunctivitis transmission: mathematical modeling insights from kenya. 2024.

[3] C. S. Chou and A. Friedman. *Introduction to mathematical biology*. 2010.

[4] E. K. Yeargers, J. V. Herod, and R. W. Shonkweiler. *An introduction to the mathematics of biology: with computer algebra models*. Springer Science & Business Media, 2013.

[5] J. D. Murray. Vignettes from the field of mathematical biology: the application of mathematics to biology and medicine. *Interface Focus*, 2(4):397–406, 2012.

[6] S. N. Kyere, F. A. Boateng, G. F. Hoggar, and P. Jonathan. Optimal control model of haemorrhagic conjunctivitis disease. *Adv. Comput. Sci.*, 1(2):108, 2012.

[7] Zeeshan M. Ayaz H. Iqbal A. Ali F. Nawaz, S. and A. Ali. The outbreak of highly contagious conjunctivitis (pink eye) in major cities of pakistan. *The Open Infectious Diseases Journal*, 16(1):2024, 2024.

[8] S. R. Fehily, G. B. Cross, and A. J. Fuller. Bilateral conjunctivitis in a returned traveller. *PLoS Neglected Tropical Diseases*, 9(1):e0003351, 2015.

[9] R. H. Elliot. Conjunctivitis in the tropics. *British Medical Journal*, 1(12):3340, 1925.

[10] O. Ghazali, K. B. Chua, K. P. Ng, P. S. Hooi, M. A. Pallansch, M. S. Oberste, and J. W. Mak. *An outbreak of acute haemorrhagic conjunctivitis in Melaka, Malaysia*, volume 44. 2003.

[11] J. Chansaenroj, S. Vongpunsawad, J. Puenpa, A. Theamboonlers, V. Vuthitanachot, P. Chattakul, and Y. Poovorawan. *Epidemic outbreak of acute haemorrhagic conjunctivitis caused by coxsackievirus A24 in Thailand, 2014*, volume 143. 2015.

[12] G. Chowell, E. Shim, F. Brauer, P. Diaz-Dueñas, J. M. Hyman, and C. Castillo-Chavez. Modelling the transmission dynamics of acute haemorrhagic conjunctivitis: application to the 2003 outbreak in mexico. *Statistics in Medicine*, 25(11):1840–1857, 2006.

[13] J. Suksawat and S. Naowarat. Effect of rainfall on the transmission model of conjunctivitis. 2014.

[14] B. Unyong and S. Naowarat. Stability analysis of conjunctivitis model with nonlinear incidence term. *Australian Journal of Basic and Applied Sciences*, 8(24):52–58, 2014.

[15] S. Sangthongjeen, A. Sudchumnong, and S. Naowarat. Effect of educational campaign on transmission model of conjunctivitis. *Australian Journal of Basic and Applied Sciences*, 9(7):811–815, 2015.

[16] M. Farman, A. Shehzad, K. S. Nisar, E. Hincal, A. Akgul, and A. M. Hassan. Generalized ulam-hyers-rassias stability and novel sustainable techniques for dynamical analysis of global warming impact on ecosystem. *Scientific Reports*, 13(1):22441, 2023.

[17] C. Xu and M. Farman. Dynamical transmission and mathematical analysis of ebola

virus using a constant proportional operator with a power law kernel. *Fractal and Fractional*, 7(10):706, 2023.

[18] A. Ahmad, K. Faiz, M. Farman, S. Sattar, and A. Sambas. Control and effect of climate change due to human activities by mathematical modeling approach under fractional operator. *Modeling Earth Systems and Environment*, 11(4):1–21, 2025.

[19] M. M. Matar, M. I. Abbas, J. Alzabut, M. K. A. Kaabar, S. Etemad, and S. Rezapour. Investigation of the p-laplacian nonperiodic nonlinear boundary value problem via generalized caputo fractional derivatives. *Advances in Difference Equations*, pages 1–18, 2021.

[20] M. Farman, A. Ahmad, A. Zehra, K. S. Nisar, E. Hincal, and A. Akgul. Analysis and controllability of diabetes model for experimental data by using fractional operator. *Mathematics and Computers in Simulation*, 218:133–148, 2024.

[21] M. Tashfeen, H. S. Jassim, F. Dayan, M. A. Rehman, A. D. ZoltÃ¡n, and H. A. Neamah. An analytical approach to modeling conjunctival viral disease using fuzzy logic and time-delay dynamics. *Healthcare Analytics*, page 100404, 2025.

[22] G. Dagasso, J. Urban, and M. Kwiatkowska. Incorporating time delays in the mathematical modelling of the human immune response in viral infections. *Procedia Computer Science*, 185:144–151, 2021.

[23] S. Mehnaz, M. N. Khan, I. Ahmad, S. Abdel-Khalek, A. M. Alghamdi, and M. Inc. The generalized time fractional gardner equation via numerical meshless collocation method. *Thermal Science*, 26(Spec. issue 1):469–474, 2022.

[24] S. Alyobi and R. Jan. Qualitative and quantitative analysis of fractional dynamics of infectious diseases with control measures. *Fractal and Fractional*, 7(5):400, 2023.

[25] M. Caputo. Linear models of dissipation whose q is almost frequency independentii. *Geophysical Journal International*, 13(5):529–539, 1967.

[26] A. M. Kimulu, W. N. Mutuku, S. M. Mwalili, D. Malonza, and A. S. Oke. Mathematical modelling of the effects funding on hiv dynamics among truckers and female sex workers along the kenyan northern corridor highway. 2022.

[27] A. Atangana. Mathematical model of survival of fractional calculus, critics and their impact: How singular is our world? *Advances in Difference Equations*, (403), 2021.

[28] S. Sangsawang, T. Tanutpanit, W. Mumtong, and P. Pongsumpun. Local stability analysis of mathematical model for hemorrhagic conjunctivitis disease. *KMITL Science and Technology Journal*, 12(2):189–197, 2012.

[29] P. Van den Driessche and J. Watmough. Reproduction numbers and sub-threshold endemic equilibria for compartmental models of disease transmission. *Mathematical Biosciences*, 180(1-2):29–48, 2002.

[30] Kulachi M. O. Aly A. A. Inc M. Ahmad M. O. Ahmad, A. and S. Rezapour. Flip bifurcation analysis and investigation of conjunctivitis virus by using sustainable control approach. *Biomedical Signal Processing and Control*, 100:106956, 2025.

[31] S. Gandon, M. Mackinnon, S. Nee, and A. Read. Imperfect vaccination: some epidemiological and evolutionary consequences. *Proceedings of the Royal Society of London. Series B: Biological Sciences*, 270(1520):1129–1136, 2003.

[32] A. Atangana and A. Akgül. On solutions of fractal fractional differential equations.

Discrete & Continuous Dynamical Systems - Series S, 14(10), 2021.

[33] M. Caputo and M. Fabrizio. A new definition of fractional derivative without singular kernel. *Progress in Fractional Differentiation & Applications*, 1(2):73–85, 2015.

[34] I. Podlubny. *Fractional Differential Equations*. Mathematics in Science and Engineering. 1999.

[35] M. Farman, K. S. Nisar, A. Shehzad, D. Baleanu, A. Amjad, and F. Sultan. Computational analysis and chaos control of the fractional order syphilis disease model through modeling. *Ain Shams Engineering Journal*, 15(6):102743, 2024.

[36] S. Nana-Kyere, D. T. Banon, S. N. Marmah, and D. Kwarteng. Stochastic optimal control model of haemorrhagic conjunctivitis disease. *Journal of Advances in Mathematics and Computer Science*, 31(3):1–19, 2019.